

Effective Temperatures and Radiation Spectra for a Higher-Dimensional Schwarzschild-de-Sitter Black-Hole

P. Kanti and T. Pappas

*Division of Theoretical Physics, Department of Physics,
University of Ioannina, Ioannina GR-45110, Greece*

Abstract

The absence of a true thermodynamical equilibrium for an observer located in the causal area of a Schwarzschild-de Sitter spacetime has repeatedly raised the question of the correct definition of its temperature. In this work, we consider five different temperatures for a higher-dimensional Schwarzschild-de Sitter black hole: the bare T_0 , the normalised T_{BH} and three effective ones given in terms of both the black hole and cosmological horizon temperatures. We find that these five temperatures exhibit similarities but also significant differences in their behaviour as the number of extra dimensions and the value of the cosmological constant are varied. We then investigate their effect on the energy emission spectra of Hawking radiation. We demonstrate that the radiation spectra for the normalised temperature T_{BH} – proposed by Bousso and Hawking over twenty years ago – leads to the dominant emission curve while the other temperatures either support a significant emission rate only at a specific Λ regime or they have their emission rates globally suppressed. Finally, we compute the bulk-over-brane emissivity ratio and show that the use of different temperatures may lead to different conclusions regarding the brane or bulk dominance.

1 Introduction

The novel theories, that postulate the existence of additional spacelike dimensions in nature [1, 2] with size much larger than the Planck length or even infinite, have in fact an almost 20-year life-time. During that period, several aspects of gravity, cosmology and particle physics have been reconsidered in the context of these higher-dimensional theories. Black hole solutions have been intensively studied since the existence of extra dimensions affects both their creation and decay processes (for more information on this, one may consult the reviews [3]-[14]).

The presence of the brane(s) in the model with warped extra dimensions [2] has proven so far to be an unsurmountable obstacle for the construction of analytical solutions describing regular black holes. As a result, most of the study of the decay process of a higher-dimensional black hole has been restricted in the context of the model with large extra dimensions [1], where the latter are assumed to be empty, and thus flat, and where the self-energy of the brane may be ignored compared to the black-hole mass. It is in the context of this theory that analytical expressions describing higher-dimensional black holes may be written, and the emission of particles, comprising the Hawking radiation [15], may be studied in detail.

Historically, the first solution describing a higher-dimensional, spherically-symmetric black hole appeared in the '60s, and is known as the Tangherlini solution [16]. The solution describes a higher-dimensional analogue of the Schwarzschild solution of the General Theory of Relativity that is formed also in the presence of a cosmological constant. Therefore, this solution constitutes in fact an improvement of the assumption made in the context of the large extra dimensions scenario where the extra space is absolutely empty: here, the extra dimensions are filled with a constant distribution of energy, or with some field configuration that effectively acts as a constant distribution of energy. For a positive cosmological constant, the solution describes a higher-dimensional Schwarzschild-de Sitter black-hole spacetime.

Although the emission of Hawking radiation from higher-dimensional, spherically-symmetric or rotating black holes has been extensively studied in the literature (for a partial only list see [17]-[37] or the aforementioned reviews [3]-[14]), the analyses focused on the higher-dimensional Schwarzschild-de Sitter black holes are only a few. The first such work [38] contained an analytic study of the greybody factor for scalar fields propagating on the brane and in the bulk, and in addition provided exact numerical results for the radiation spectra in both emission channels. A subsequent analytic work [39] extended the aforementioned analysis by determining the next-to-leading-order term in the expansion of the greybody factor. An exact numerical study [40] then considered the emission of fields with arbitrary spin from a higher-dimensional Schwarzschild-de Sitter black hole. A series of three, more recent works studied the case of a scalar field having a non-minimal coupling to the scalar curvature: the first [41] studied the case of a purely 4-dimensional Schwarzschild-de Sitter black hole, the second [42] considered the scalar field propagating either in the higher-dimensional bulk or being restricted on a brane, and a third one [43] provided exact numerical results for the greybody factors and radiation spectra in the same theory. A few additional works [44, 45, 46, 47, 48] have also

appeared that studied the greybody factors for fields propagating in the background of variants of a Schwarzschild-de-Sitter black hole.

However, over the years, the question of what is the correct notion of the temperature of a Schwarzschild - de Sitter (SdS) spacetime has risen. This spacetime contains a black hole whose event horizon sets the lower boundary of the causally connected spacetime. But it also contains a positive cosmological constant that gives rise to a cosmological horizon, the upper boundary of the causal spacetime. An observer living at any point of this causal area is never in a true thermodynamical equilibrium - the two horizons have each one its own temperature, expressed in terms of their surface gravities [49, 50], and thus an incessant flow of thermal energy (from the hotter black-hole horizon to the colder cosmological one) takes place at every moment. In addition, the SdS spacetime lacks an asymptotically-flat limit where the black-hole parameters may be defined in a robust way. The latter problem was solved in [51] where a *normalised* black-hole temperature was proposed that made amends for the lack of an asymptotic limit. Then, assuming that the value of the cosmological constant is small and the two horizons are thus located far away from each other, one could formulate two independent thermodynamics.

Despite the above, the question of what happens as the cosmological constant becomes larger and the two horizons come closer still persisted. It was this question that gave rise to the notion of the *effective temperature* for an SdS spacetime [52, 53, 54, 55, 56], namely one that implements both the black-hole and the cosmological horizon temperatures (for a review on this, see [57]). A number of additional works have appeared in the literature with similar or alternative approaches on the thermodynamics of de Sitter spacetimes [58]-[76], however, the question of the appropriate expression of the SdS black-hole temperature still remains open.

Up to now, no work has appeared in the literature that makes a comprehensive study of the different temperatures for an SdS spacetime and compare their predictions for the corresponding Hawking radiation spectra. In fact, previous works that study the radiation spectra from a four-dimensional or higher-dimensional SdS black hole make use of either its *bare* temperature T_0 , based on its surface gravity, or the normalised one T_{BH} , at will. In the context of this work, we will perform such a comprehensive study, and we will derive and compare the derived radiation spectra. We will do so not only for the aforementioned two SdS black-hole temperatures but also for three additional effective temperatures for the SdS spacetime, namely T_{eff-} , T_{eff+} and T_{effBH} – the use of one of the latter temperatures may be unavoidable for large values of the cosmological constant when the two horizons lie so close that the independent thermodynamics no longer hold. To address the above, we will also extend the regime of values of the cosmological constant that has been studied in the literature so far, and consider the entire allowed regime, from a very small value up to its maximum critical value [77].

To make our analysis as general as possible, we will consider a higher-dimensional SdS spacetime. We will then study the properties of the different temperatures both in terms of the value of the cosmological constant but also of the number of extra spacelike dimensions. The corresponding Hawking radiation spectra will then be produced for scalar fields, both minimally and non-minimally coupled to gravity, propagating either on our brane or in the bulk. As we will see, the different temperatures will lead to different

energy emission rates for the black hole, each one with its own profile in terms of the bulk cosmological constant, number of extra dimensions and value of the non-minimal coupling constant. In addition, each temperature will lead to different conclusions regarding the dominance of the brane or of the bulk.

The outline of our paper is as follows: in Section 2, we present the theoretical framework of our analysis, the gravitational background, the equations of motion for the scalar field as well as the different definitions of the temperature of an SdS spacetime. In Sections 3 and 4, we derive the energy emission rates for bulk and brane scalar fields, having a minimal or non-minimal coupling to gravity, respectively. In Section 5, we calculate the bulk-over-brane emissivity ratio and, in Section 6, we summarise our analysis and present our conclusions.

2 The Theoretical Framework

2.1 The Gravitational Background

We will start by considering a higher-dimensional gravitational theory with $D = 4 + n$ total number of dimensions. The action functional of the theory will also contain a positive cosmological constant Λ , and will therefore read

$$S_D = \int d^{4+n}x \sqrt{-G} \left(\frac{R_D}{2\kappa_D^2} - \Lambda \right). \quad (1)$$

In the above, R_D is the higher-dimensional Ricci scalar and $\kappa_D^2 = 1/M_*^{2+n}$ the higher-dimensional gravitational constant associated with the fundamental scale of gravity M_* . If we vary the above action with respect to the metric tensor G_{MN} , we obtain the Einstein's field equations that have the form

$$R_{MN} - \frac{1}{2} G_{MN} R_D = \kappa_D^2 T_{MN} = -\kappa_D^2 G_{MN} \Lambda, \quad (2)$$

with the only contribution to the energy-momentum tensor T_{MN} coming from the bulk cosmological constant.

The above set of equations admit a spherically-symmetric solution of the form [16]

$$ds^2 = -h(r) dt^2 + \frac{dr^2}{h(r)} + r^2 d\Omega_{2+n}^2, \quad (3)$$

where $d\Omega_{2+n}^2$ is the area of the $(2 + n)$ -dimensional unit sphere given by

$$d\Omega_{2+n}^2 = d\theta_{n+1}^2 + \sin^2 \theta_{n+1} \left(d\theta_n^2 + \sin^2 \theta_n \left(\dots + \sin^2 \theta_2 (d\theta_1^2 + \sin^2 \theta_1 d\varphi^2) \dots \right) \right), \quad (4)$$

with $0 \leq \varphi < 2\pi$ and $0 \leq \theta_i \leq \pi$, for $i = 1, \dots, n + 1$. The radial function $h(r)$ is found to have the explicit form [16]

$$h(r) = 1 - \frac{\mu}{r^{n+1}} - \frac{2\kappa_D^2 \Lambda r^2}{(n+3)(n+2)}. \quad (5)$$

The above gravitational background describes a $(4 + n)$ -dimensional Schwarzschild-de Sitter (SdS) spacetime, with the parameter μ related to the black-hole mass M through the relation [78]

$$\mu = \frac{\kappa_D^2 M}{(n+2)} \frac{\Gamma[(n+3)/2]}{\pi^{(n+3)/2}}. \quad (6)$$

The horizons of the SdS black hole follows from the equation $h(r) = 0$ – this has, in principle, $(n+3)$ roots, however, not all of them are real and positive; in fact, the SdS spacetime may have two, one or zero horizons, depending on the values of the parameters M and Λ [79]. Here, we will ensure that the values of M and Λ are in the regime that supports the existence of two horizons, the black-hole r_h and the cosmological one r_c , with $r_h < r_c$. However, the degenerate case, that results in the Nariai limit [77] in which the two horizons coincide, will also be investigated.

The higher-dimensional background (3) is seen by gravitons and particles with no Standard-Model quantum numbers that may propagate in the bulk. All ordinary particles, however, are restricted to live on our 4-dimensional brane [1, 2], and therefore propagate on a different gravitational background. The latter follows by projecting the $(4 + n)$ -dimensional background (3) on the brane and it is realised by fixing the value of the extra angular coordinates, $\theta_i = \pi/2$, for $i = 2, \dots, n+1$. Then, we obtain the 4D line-element

$$ds^2 = -h(r) dt^2 + \frac{dr^2}{h(r)} + r^2 (d\theta^2 + \sin^2 \theta d\varphi^2), \quad (7)$$

with the metric function $h(r)$ preserving its form, given by Eq. (5), and thus its dependence on both the number of additional spacelike coordinates n and the value of the bulk cosmological constant Λ .

2.2 The Temperature of the Schwarzschild-de Sitter Black Hole

The temperature of a black hole is traditionally defined in terms of its surface gravity k_h at the location of the horizon [49, 50]. The latter quantity is expressed as

$$k_h^2 = -\frac{1}{2} \lim_{r \rightarrow r_h} (D_M K_N)(D^M K^N), \quad (8)$$

where D_M is the covariant derivative and

$$K = \gamma_t \frac{\partial}{\partial t} \quad (9)$$

is the timelike Killing vector with γ_t a normalization constant. In the case that the gravitational background is spherically-symmetric, Eq. (8) takes the simpler form [80]

$$k_h = \frac{1}{2} \frac{1}{\sqrt{-g_{tt}g_{rr}}} |g_{tt,r}|_{r=r_h}. \quad (10)$$

When the above expression is employed for the line-element (3) of a higher-dimensional Schwarzschild-de Sitter black hole, we obtain the following expression for its temperature [49, 80, 38]

$$T_0 = \frac{k_h}{2\pi} = \frac{1}{4\pi r_h} \left[(n+1) - (n+3) \tilde{\Lambda} r_h^2 \right], \quad (11)$$

where we have defined, for convenience, the quantity $\tilde{\Lambda} = 2\kappa_D^2\Lambda/(n+2)(n+3)$, and used the condition $f(r_h) = 0$ to replace μ in terms of r_h and $\tilde{\Lambda}$.

The Schwarzschild-de Sitter spacetime is characterized, in the most generic case, by the presence of a second horizon, the cosmological horizon r_c . As a result, one may define another surface gravity k_c , this time at the location of r_c , and a temperature for the cosmological horizon [49, 50], namely [38]

$$T_c = -\frac{k_c}{2\pi} = -\frac{1}{4\pi r_c} \left[(n+1) - (n+3)\tilde{\Lambda}r_c^2 \right], \quad (12)$$

where care has been taken so that T_c is positive-definite since $r_h < r_c$ [38]. The presence of the second horizon with its own temperature makes the thermodynamics of the Schwarzschild-de Sitter spacetime significantly more complicated, as compared to the cases of either asymptotically Minkowski or Anti de Sitter spacetimes [57]. The two temperatures, T_0 and T_c , are in principle different, therefore an observer located at an arbitrary point of the causal region $r_h < r < r_c$ is not in thermodynamical equilibrium. The usual approach adopted in the literature is to make the assumption that the two horizons are located far away and therefore each one can have its own independent thermodynamics [50, 51, 62] – this assumption, however, is valid only for small values of the cosmological constant and thus it imposes a constraint on all potential analyses.

In [51], a modified expression for the temperature of the black hole was proposed, namely

$$T_{BH} = \frac{1}{\sqrt{h(r_0)}} \frac{1}{4\pi r_h} \left[(n+1) - (n+3)\tilde{\Lambda}r_h^2 \right], \quad (13)$$

in which a normalization factor $\sqrt{h(r_0)}$ was introduced involving the value of the metric function at its global maximum r_0 . This point follows from the condition $h'(r) = 0$ and is given by [38]

$$r_0^{n+3} = \frac{(n+1)\mu}{2\tilde{\Lambda}}. \quad (14)$$

There, the metric function assumes the value

$$h(r_0) = 1 - \frac{\mu}{r_0^{n+1}} - \tilde{\Lambda}r_0^2 = \frac{1}{n+1} \left[(n+1) - (n+3)\tilde{\Lambda}r_0^2 \right]. \quad (15)$$

The above is the maximum value that the metric function attains as it interpolates between the two zeros at the two horizons. The point r_0 is the point the closest that the Schwarzschild-de Sitter spacetime has to an asymptotically flat region: it is here that the effects of the black-hole and cosmological horizons cancel out and an observer can stay at rest [51]. Mathematically, the normalization factor $\sqrt{h(r_0)}$ appears from the normalization of the Killing vector, $K_M K^M = -1$: this condition is satisfied in asymptotically flat spacetime for $\gamma_t = 1$ but, at $r = r_0$, this factor should be $\gamma_t = 1/\sqrt{h(r_0)}$.

Including this normalisation factor in Eq. (13) is a step forward in defining the black-hole temperature in a non-asymptotically flat spacetime, however, this factor modifies significantly the properties of T_0 . In Fig. 1(a,b), we depict the dependence of the two

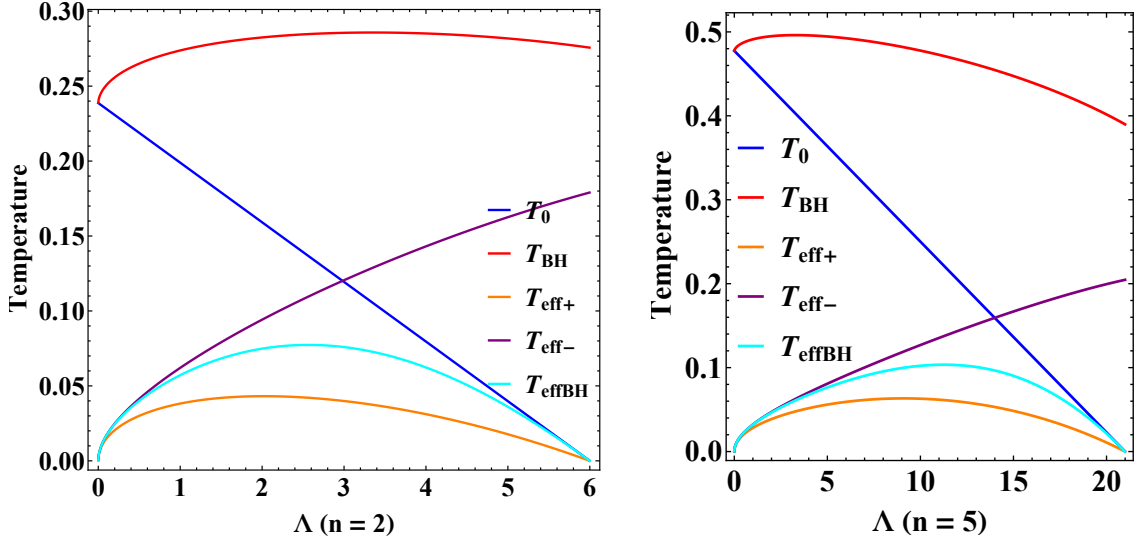


Figure 1: Temperatures for a $(4 + n)$ -dimensional Schwarzschild-de Sitter black hole as a function of the cosmological constant Λ , for: **(a)** $n = 2$, and **(b)** $n = 5$.

temperatures, T_0 and T_{BH} , as a function of the cosmological constant, and for two values of the number of extra dimensions, $n = 2$ and $n = 5$. For low n , as Λ increases, T_0 monotonically decreases, in accordance to Eq. (11), whereas T_{BH} predominantly increases - the latter is caused by the variation in the value of $h(r_0)$ that, in most part of the allowed Λ regime, causes an enhancement in T_{BH} . For large values of n , the monotonic decrease of T_0 remains unaffected while the increase of T_{BH} holds only for the lower range of values of Λ . Even in this case, the value of T_{BH} is constantly larger than that of T_0 (see, also, [40] for a similar comparison and conclusions). The two temperatures match only in the limit $\Lambda \rightarrow 0$ when they reduce to the temperature of a higher-dimensional Schwarzschild black hole. A radically different behaviour appears in the opposite limit, the Nariai or extremal limit [58, 59, 77]: as Λ approaches its maximum allowed value, the two horizons approach each other and eventually coincide, with $r_h = r_c$. In that limit, the combination inside the square brackets in Eq. (11), and thus T_0 itself, vanishes¹, a feature that is clearly shown in Fig. 1. On the contrary, in the critical limit, T_{BH} assumes an asymptotic constant value; this is caused by the fact that its numerator and denominator both tend to zero values with the ratio approaching a constant number.

In Fig. 2, we show the dependence of T_0 and T_{BH} on the number of extra dimensions n , for two different fixed values of the cosmological constant, $\Lambda = 0.1$ and $\Lambda = 0.8$ (we have set for simplicity $\kappa_D^2 = 1$, therefore Λ is given in units of r_h^{-2}). We observe again that the ‘normalised’ temperature T_{BH} remains always larger than the ‘bare’ one T_0 , however this dominance gets softer as n increases, and almost disappears for small values of Λ .

The temperature of a black hole is one of the important factors that determine the

¹Although, for arbitrary n , this is very difficult to prove analytically, for special values of n we may easily confirm it: for $n = 0$, the Nariai limit is reached when $M^2\Lambda = 1/9$ and then $r_h^2 = 1/\Lambda$; for $n = 1$, the two horizons coincide when $\mu\tilde{\Lambda} = 1/4$ and then $r_h^2 = 1/(2\tilde{\Lambda})$. In both cases, we may easily see that Eq. (11) vanishes. For higher values of n , the vanishing of Eq. (11) may be easily confirmed numerically.

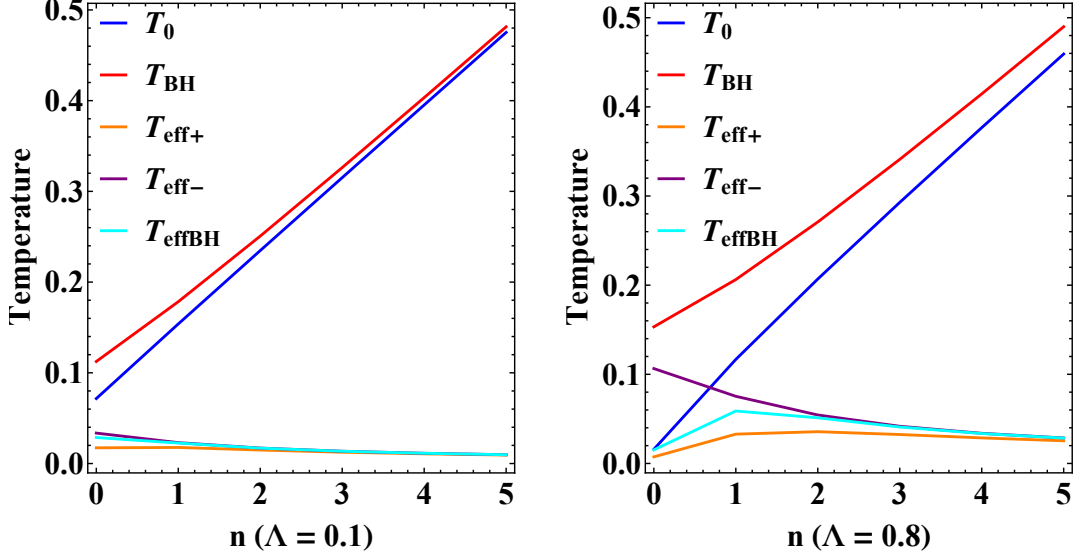


Figure 2: Temperatures for a $(4 + n)$ -dimensional Schwarzschild-de Sitter black hole as a function of the number of extra dimensions n , for: (a) $\Lambda = 0.1$, and (b) $\Lambda = 0.8$.

Hawking radiation emission spectra. Only a handful of works exist in the literature that study the emission of Hawking radiation from a Schwarzschild-de Sitter black hole, either 4-dimensional or higher-dimensional, and these use both definitions of its temperature, Eq. (11) [41, 81] or Eq. (13) [38, 40, 43], at will. In addition, during the recent years, the notion of the *effective temperature* of the Schwarzschild-de Sitter spacetime has emerged, that involves both temperatures T_0 and T_c , in an attempt to unify the thermodynamical description of this spacetime. In the most popular of the analyses, a thermodynamical first law for a Schwarzschild-de Sitter black hole is written in which the black-hole mass plays the role of the enthalpy of the system ($M = -H$), the cosmological constant that of the pressure ($P = \Lambda/8\pi$) while the entropy is the sum of the entropies of the two horizons ($S = S_h + S_c$) [52, 53, 54, 55, 56, 57]. In this picture, an effective temperature emerges that has the form

$$T_{\text{eff}-} = \left(\frac{1}{T_c} - \frac{1}{T_0} \right)^{-1} = \frac{T_0 T_c}{T_0 - T_c}. \quad (16)$$

The above expression was obtained for the case of a 4-dimensional Schwarzschild-de Sitter black hole. However, the arguments leading to the formulation of the aforementioned first thermodynamical law had no explicit dependence on the dimensionality of spacetime. Therefore, we expect that the functional form of the effective temperature $T_{\text{eff}-}$ for the case of a $(4 + n)$ -dimensional Schwarzschild-de Sitter black hole will still be given by Eq. (16), but with the individual temperatures T_0 and T_c , now assuming their higher-dimensional forms, Eqs. (11) and (12). Then, the explicit form of $T_{\text{eff}-}$ in $D = 4 + n$ dimensions will be the following

$$T_{\text{eff}-} = -\frac{1}{4\pi} \frac{(n+1)^2 - (n+1)(n+3)\tilde{\Lambda}(r_h^2 + r_c^2) + (n+3)^2\tilde{\Lambda}^2 r_h^2 r_c^2}{(r_h + r_c)[(n+1) - (n+3)\tilde{\Lambda} r_h r_c]}. \quad (17)$$

In the limit $r_h \rightarrow 0$, the above expression for the effective temperature reduces to that of the cosmological horizon T_c , as expected. However, the limit $r_c \rightarrow \infty$ (or, equivalently, $\tilde{\Lambda} \rightarrow 0$) leads to a vanishing result: the effective temperature does not interpolate between the black-hole temperature T_0 and the cosmological one T_c , as one may have expected; in fact, the limit $\Lambda \rightarrow 0$ is a particular one since it is equivalent to a vanishing pressure of the system, that in the relevant analyses is always assumed to be positive. That is, by construction, T_{eff-} is valid for non-vanishing cosmological constant - but this is exactly the regime where the need for an effective temperature really emerges since, in the limit of small Λ , the horizons r_h and r_c are located so far away from each other that the independent thermodynamics at the two horizons do indeed hold.

In Figs. 1 and 2, we depict also the behaviour of T_{eff-} in terms of the value of the cosmological constant Λ and the number of extra dimensions n , respectively. The effective temperature T_{eff-} is an increasing function of Λ , and, similarly to the case of the normalised temperature T_{BH} , it assumes a non-vanishing constant value at the critical limit - as in the case of T_{BH} , the numerator and denominator of Eq. (16) both go to zero with their ratio tending to a constant number. On the contrary, T_{eff-} is a decreasing function of the number of extra dimensions n .

The effective temperature T_{eff-} was found to exhibit some unphysical properties, especially in the case of charged de Sitter black holes where the aforementioned expression may take on negative values or exhibit infinite jumps at the critical point. For this reason, in [57] (see also [52]) a new expression for the effective temperature of a Schwarzschild-de Sitter spacetime was proposed, namely the following

$$T_{eff+} = \left(\frac{1}{T_c} + \frac{1}{T_0} \right)^{-1} = \frac{T_0 T_c}{T_0 + T_c}. \quad (18)$$

The above proposal was characterised as an ‘ad hoc’ one, that would follow from an analysis similar to that leading to T_{eff-} in which the entropy of the system would be the difference of the entropies of the two horizons, i.e. $S = S_c - S_h$, instead of their sum. In the higher-dimensional case, the aforementioned alternative effective temperature has the explicit form

$$T_{eff+} = \frac{1}{4\pi} \frac{(n+1)^2 - (n+1)(n+3)\tilde{\Lambda}(r_h^2 + r_c^2) + (n+3)^2\tilde{\Lambda}^2 r_h^2 r_c^2}{(r_h - r_c) [(n+1) + (n+3)\tilde{\Lambda} r_h r_c]}. \quad (19)$$

In the limit $r_h \rightarrow 0$, T_{eff+} reduces again to T_c . When $\Lambda \rightarrow 0$, it also exhibits the same behaviour as T_{eff-} by going to zero. However, near the critical point, T_{eff+} has a distinct behaviour as it vanishes instead of taking a constant value. This is in accordance with Eq. (18) where the numerator clearly approaches zero faster than the denominator. It is perhaps the vanishing of T_{eff+} near the critical point that helps to avoid the infinite jumps and makes this alternative effective temperature more physically acceptable. The complete behaviour of T_{eff+} in terms of the cosmological constant is depicted in Fig. 1; its decreasing behaviour in terms of n is also shown in Fig. 2.

Inspired by the above analysis, here we propose a third, alternative form for the effective temperature of a Schwarzschild-de Sitter spacetime. Its functional form is the

following

$$T_{effBH} = \left(\frac{1}{T_c} - \frac{1}{T_{BH}} \right)^{-1} = \frac{T_{BH}T_c}{T_{BH} - T_c}, \quad (20)$$

and it matches the one of T_{eff-} , but with the normalised black-hole temperature T_{BH} in the place of the bare one T_0 . Our proposal may be considered as an equally ‘ad hoc’ one compared to that of (18); however, T_{effBH} would follow from exactly the same analysis that gave rise to T_{eff-} (with $S = S_h + S_c$) with the only difference being the consideration that the ‘correct’ black-hole temperature, due to the absence of asymptotic flatness, is T_{BH} instead of T_0 . Its explicit form in a spacetime with $D = 4 + n$ dimensions is

$$T_{effBH} = -\frac{1}{4\pi} \frac{(n+1)^2 - (n+1)(n+3)\tilde{\Lambda}(r_h^2 + r_c^2) + (n+3)^2\tilde{\Lambda}^2 r_h^2 r_c^2}{(r_h \sqrt{h(r_0)} + r_c) [(n+1) - (n+3)\tilde{\Lambda} r_h r_c]}. \quad (21)$$

The above definition shares many characteristics with the effective temperature T_{eff-} : it also reduces to T_c when $r_h \rightarrow 0$ and it vanishes in the limit $\Lambda \rightarrow 0$. But it also exhibits the same attractive behaviour near the critical point as T_{eff+} by going to zero; this is due to the fact that, as we approach the critical point, T_{BH} in Eq. (20) is a constant while T_c vanishes. The complete profile of T_{effBH} as a function of the cosmological constant is depicted in Fig. 1, while its similar behaviour in terms of n , compared to the other effective temperatures, is shown in Fig. 2. Observing Fig. 1, it is interesting to note that T_{effBH} matches T_{eff-} over an extended low Λ -regime, and then coincides with T_0 in the high Λ -regime².

3 Hawking Radiation for Minimally-Coupled Scalar Fields

In the previous section, we examined in detail the characteristics of two temperatures for the Schwarzschild-de Sitter black hole, the bare T_0 and the normalised one T_{BH} , as well as three effective temperatures for the Schwarzschild-de Sitter spacetime, T_{eff-} , T_{eff+} and T_{effBH} , to which the SdS black hole belongs. In this section, we proceed to derive and compare the radiation spectra for scalar fields emitted by the SdS black hole, for each one of the aforementioned five temperatures.

Our analysis will focus on the higher-dimensional case and will present radiation spectra for scalar fields emitted both on the brane and in the bulk. To this end, we need also the greybody factor for brane and bulk scalar fields propagating in the SdS background. These have been derived analytically, in the limit of small cosmological constant, in [42] and numerically, for arbitrary values of Λ , in [43]. Since here we are interested in deriving the form of the spectra for the complete range of Λ , we will use the exact results derived in [43]. For the sake of completeness, we will briefly review

²One may wonder whether an alternative effective temperature could be defined along the lines of Eq. (20) but with a normalised temperature for the cosmological horizon too, i.e. $T_{cBH} = T_c/\sqrt{h(r_0)}$. As one may see, such a temperature would have a similar behaviour to T_{eff-} in the small Λ -regime but would have an ill-defined behaviour near the critical point where it diverges.

the method for calculating the scalar greybody factors in a SdS spacetime - for more information, interested readers may look in [43].

We will start from the emission of scalar fields on the brane. The equation of motion of a free, massless scalar field minimally-coupled to gravity and propagating in the brane background (7) has the form

$$\frac{1}{\sqrt{-g}} \partial_\mu (\sqrt{-g} g^{\mu\nu} \partial_\nu \Phi) = 0. \quad (22)$$

If we assume a factorized ansatz for the field, i.e. $\Phi(t, r, \theta, \varphi) = e^{-i\omega t} R(r) Y(\theta, \varphi)$, where $Y(\theta, \varphi)$ are the usual scalar spherical harmonics, we obtain a radial equation for the function $R(r)$ of the form

$$\frac{1}{r^2} \frac{d}{dr} \left(h r^2 \frac{dR}{dr} \right) + \left[\frac{\omega^2}{h} - \frac{l(l+1)}{r^2} \right] R = 0. \quad (23)$$

As was shown in [43], in the near-horizon regime, the above equation takes the form of a hypergeometric equation. Its solution, when expanded in the limit $r \rightarrow r_h$ takes the form of an ingoing free wave, namely

$$R_{BH} \simeq A_1 f^{\alpha_1} = A_1 e^{-i(\omega r_h/A_h) \ln f}, \quad (24)$$

where $A(r) = (n+1) - (n+3) \tilde{\Lambda} r^2$ and $A_h = A(r = r_h)$. Also, f is a new radial variable defined through the relation

$$r \rightarrow f(r) = \frac{h(r)}{1 - \tilde{\Lambda} r^2}. \quad (25)$$

For simplicity, we may appropriately choose the arbitrary constant A_1 so that

$$R_{BH}(r_h) = 1. \quad (26)$$

The above expression serves as a boundary condition for the numerical integration of Eq. (23). The second boundary condition comes from the near-horizon value of the first derivative of the radial function (24) for which we obtain [43]

$$\left. \frac{dR_{BH}}{dr} \right|_{r_h} \simeq -\frac{i\omega}{h(r)}. \quad (27)$$

Near the cosmological horizon, the radial equation (23) takes again the form of a hypergeometric differential equation whose general solution, in the limit $r \rightarrow r_c$ and $f \rightarrow 0$, is written as [42, 43]

$$R_C \simeq B_1 e^{-i(\omega r_c/A_c) \ln f} + B_2 e^{i(\omega r_c/A_c) \ln f}, \quad (28)$$

In the above, $A_c = A(r = r_c)$, and $B_{1,2}$ are the amplitudes of the ingoing and outgoing free waves. Then, the greybody factor, or equivalently the transmission probability, for the scalar field is given by

$$|A|^2 = 1 - \left| \frac{B_2}{B_1} \right|^2. \quad (29)$$

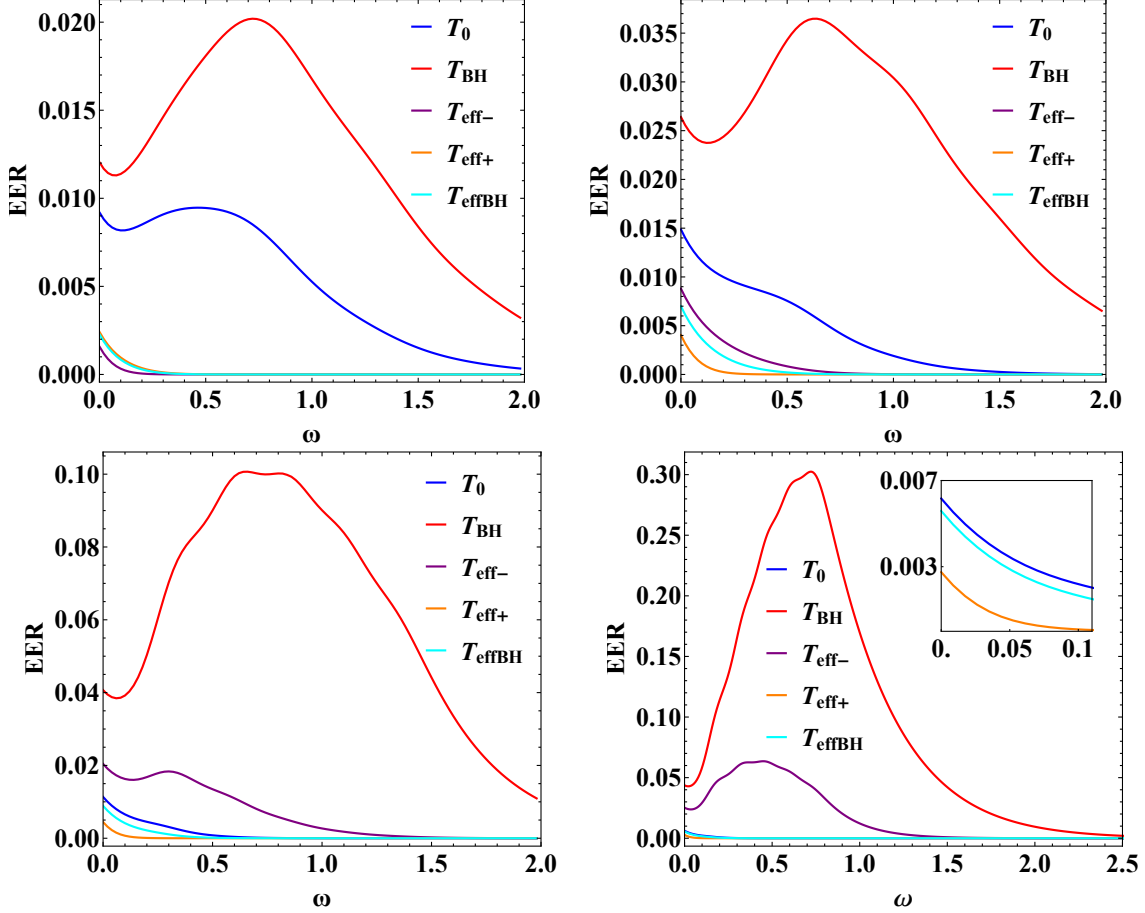


Figure 3: Energy emission rates for scalar fields on the brane from a 6-dimensional ($n = 2$) Schwarzschild-de Sitter black hole for different temperatures T , and for: (a) $\Lambda = 0.8$, (b) $\Lambda = 2$, (c) $\Lambda = 4$, and (d) $\Lambda = 5$ (in units of r_h^{-2}).

The $B_{1,2}$ amplitudes are found by integrating numerically Eq. (23), starting close to the black-hole horizon, i.e. from $r = r_h + \epsilon$, where $\epsilon = 10^{-6} - 10^{-4}$, and proceeding towards the cosmological horizon (again, for more information on this, see [43]). The exact numerical analysis demonstrated that for a minimally-coupled, massless scalar field propagating on the brane, the greybody factor is enhanced over the whole energy regime as the cosmological constant Λ increases.

Having at our disposal the exact values of the greybody factor $|A|^2$, we may now proceed to derive the differential energy emission rate for brane scalars. This is given by the expression [18, 3, 38]

$$\frac{d^2 E}{dt d\omega} = \frac{1}{2\pi} \sum_l \frac{N_l |A|^2 \omega}{\exp(\omega/T) - 1}, \quad (30)$$

where ω is the energy of the emitted particle, and $N_l = 2l + 1$ the multiplicity of states that, due to the spherical symmetry, have the same angular-momentum number [82]. Also, T is the temperature of the black hole - this will be taken to be equal to T_0 , T_{BH} ,

T_{eff-} , T_{eff+} and T_{effBH} , respectively, in order to derive the corresponding radiation spectra. As was demonstrated in [43], the dominant modes of the scalar field are the ones with the lowest values of l - in fact, all modes higher than the $l = 7$ have negligible contributions to the total emission rate.

In Fig. 3, we depict the differential energy emission rates for a higher-dimensional Schwarzschild-de Sitter black hole for the case of $n = 2$ and for four different values of the bulk cosmological constant ($\Lambda = 0.8, 2, 4, 5$). For the first, small value of Λ , all the effective temperatures have an almost vanishing value, therefore the corresponding spectra are significantly suppressed; it is the two black-hole temperatures, T_0 and T_{BH} , that lead to significant emission rates, with the latter dominating over the former in accordance to the behaviour presented in Fig. 1. As Λ increases to the value of 2, the effective temperatures, and their corresponding spectra, start becoming important; at the same time, the emission spectrum for the bare temperature T_0 is suppressed whereas the one for the normalised T_{BH} is enhanced. For $\Lambda = 4$ and 5 finally, the radiation spectrum for T_{BH} is further enhanced while the one for T_{eff-} has also become important - it is these two temperatures that tend to a constant, non-vanishing value at the critical limit; on the contrary, all three remaining temperatures, T_0 , T_{eff+} and T_{effBH} , tend to zero thus causing a suppression to the corresponding spectra.

Let us also note that the traditional shape of the energy emission curves - starting from zero and reaching a maximum value before vanishing again - is severely distorted. The presence of the cosmological constant leads to a non-vanishing asymptotic value of the greybody factor in the limit $\omega \rightarrow 0$ [38, 39, 41, 42, 43] given by

$$|A^2| = \frac{4r_h^2 r_c^2}{(r_c^2 + r_h^2)^2} + \mathcal{O}(\omega). \quad (31)$$

The above holds for the case of minimally-coupled, massless scalar fields propagating in the brane background, and leads to a significant emission rate of extremely soft, low-energetic particles - this feature is evident in all plots of Fig. 3. In addition, when the temperature employed has a small value, like the effective temperatures in the low and intermediate Λ -regime or T_0 , T_{eff+} and T_{effBH} near the critical limit, the emission curve never reaches a maximum at an energy larger than zero; rather, it exhibits only the ‘tail’, and monotonically decreases towards zero.

The case of an even higher-dimensional Schwarzschild-de Sitter black hole with $n = 5$ is shown in Fig. 4. A similar behaviour, to the one presented in the case of $n = 2$, is also observed here: for low values of Λ , the radiation spectra for all effective temperatures are suppressed; as Λ increases, they get moderately enhanced while for large values of Λ only the one for T_{eff-} takes up significant values. The radiation spectrum for the bare temperature T_0 starts at its highest values for small Λ and is constantly suppressed as the value of the cosmological constant increases. The radiation spectrum for the normalised black-hole temperature T_{BH} is the one that dominates over the whole Λ -regime - even in the high Λ -regime, where T_{BH} is suppressed with Λ according to Fig. 1(b), the compensating enhancement of the greybody factor [43] causes the overall increase of the differential energy emission rate.

Let us also study the emission of scalar fields from a higher-dimensional Schwarz-

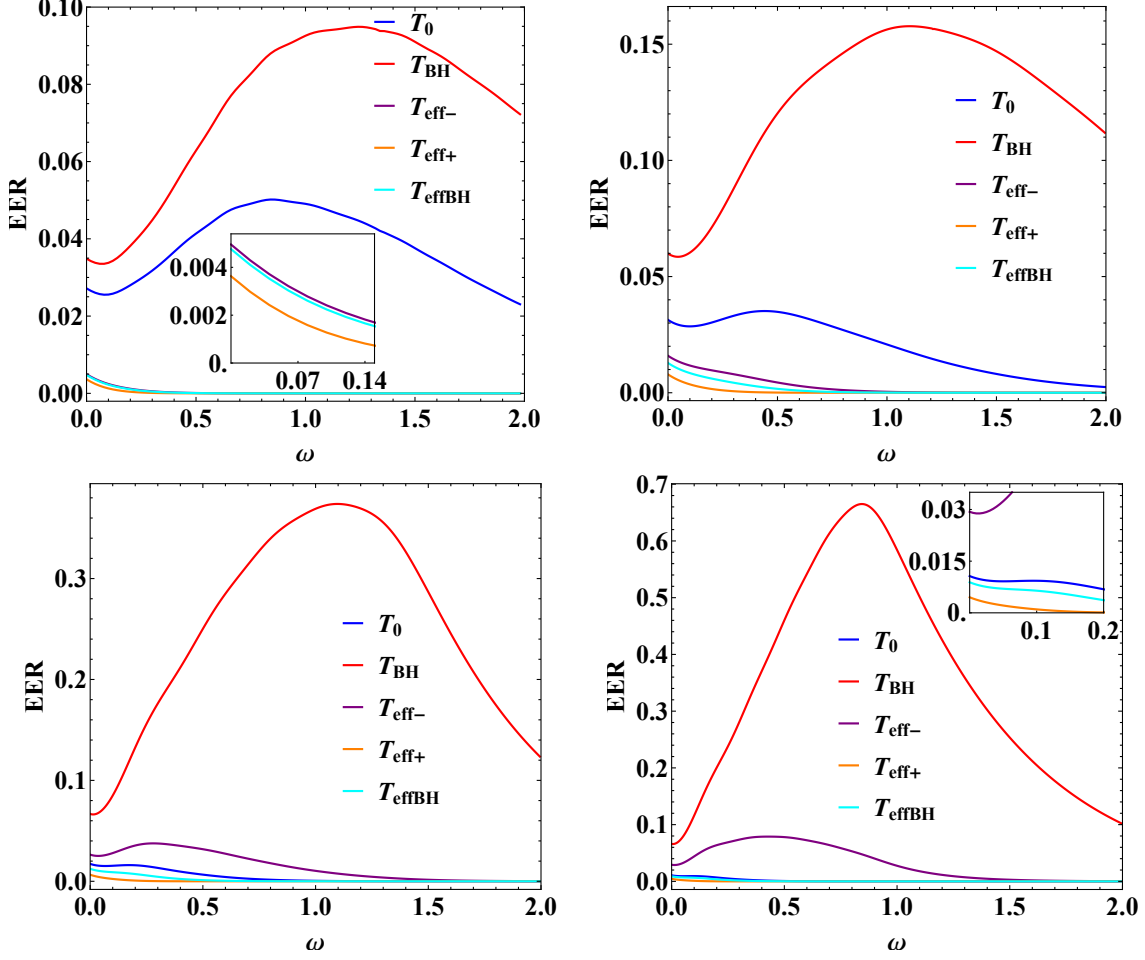


Figure 4: Energy emission rates for scalar fields on the brane from a 9-dimensional ($n = 5$) Schwarzschild-de Sitter black hole for different temperatures T , and for: **(a)** $\Lambda = 4$, **(b)** $\Lambda = 10$, **(c)** $\Lambda = 16$, and **(d)** $\Lambda = 18$ (in units of r_h^{-2}).

schild-de Sitter black hole in the bulk. The equation of motion of a free, massless field propagating in the bulk is also given by the covariant equation (22) but with the projected metric tensor $g_{\mu\nu}$ of Eq. (7) being replaced by the higher-dimensional one G_{MN} given in Eq. (3). Assuming again a factorized form $\Phi(t, r, \theta_i, \varphi) = e^{-i\omega t} R(r) \tilde{Y}(\theta_i, \varphi)$, where $\tilde{Y}(\theta_i, \varphi)$ are the hyperspherical harmonics [83], we obtain the following radial equation [42]

$$\frac{1}{r^{n+2}} \frac{d}{dr} \left(h r^{n+2} \frac{dR}{dr} \right) + \left[\frac{\omega^2}{h} - \frac{l(l+n+1)}{r^2} \right] R = 0. \quad (32)$$

The above differential equation may be again analytically solved for small Λ [42] but, for the purpose of comparing the radiation spectra over the entire Λ regime, we turn again to numerical integration. This has been performed in [43] by following an analysis similar to the one for brane scalar fields. The asymptotic solutions of Eq. (32) near the black-hole and cosmological horizons take similar forms to the brane ones, with their expanded forms (24) and (28) being identical. The same boundary conditions (26)-(27)

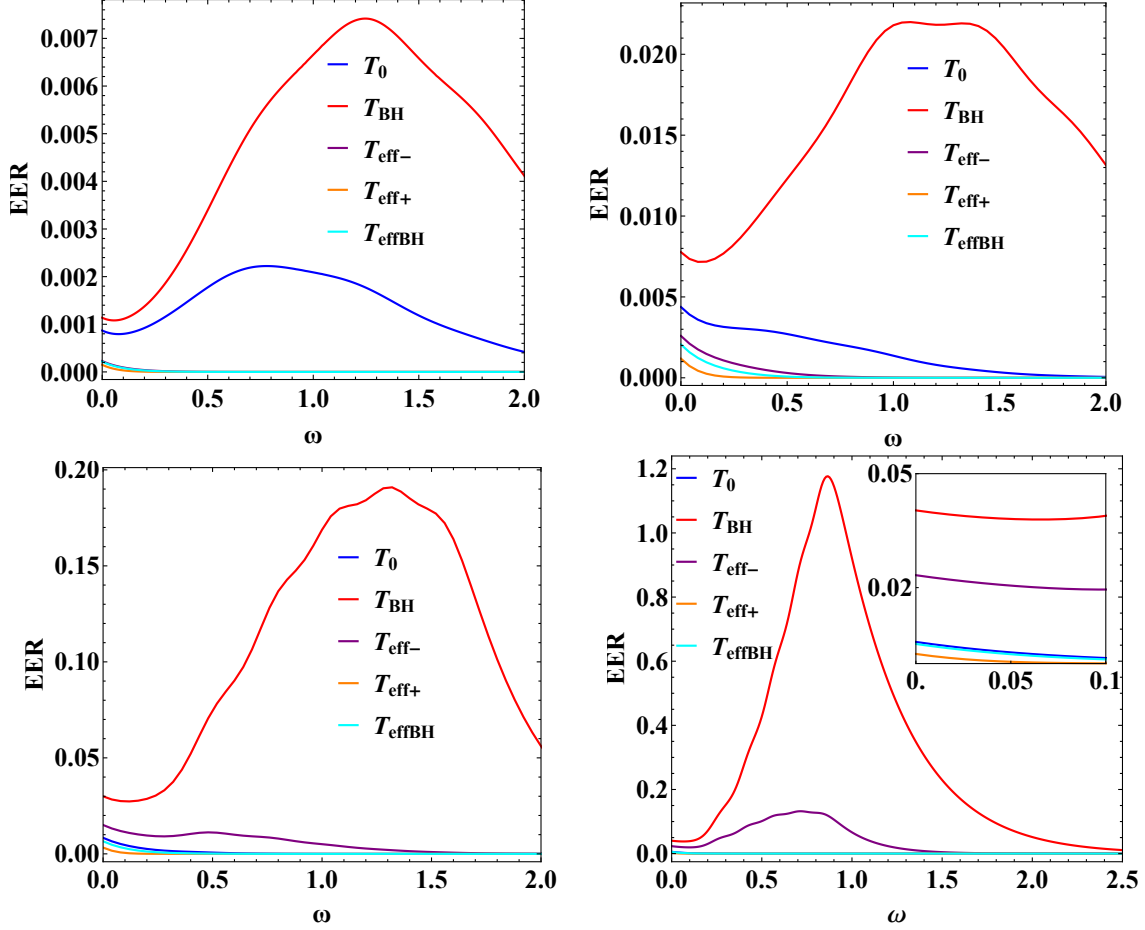


Figure 5: Energy emission rates for scalar fields in the bulk from a 6-dimensional ($n = 2$) Schwarzschild-de Sitter black hole for different temperatures T , and for: (a) $\Lambda = 0.8$, (b) $\Lambda = 2$, (c) $\Lambda = 4$, and (d) $\Lambda = 5$ (in units of r_h^{-2}).

were used for the numerical integration from the black-hole to the cosmological horizon. The exact value of the greybody factor for bulk scalar fields, for arbitrary values of the particle and spacetime parameters, was again derived via Eq. (29), and found to be an increasing function of the bulk cosmological constant.

In Fig. 5, we display the differential energy emission rates for bulk scalar fields emitted by a 6-dimensional ($n = 2$) SdS black hole, and for four different values of the cosmological constant. Similarly to the behaviour observed in the case of brane emission, the radiation spectrum for the normalised temperature T_{BH} is the one that dominates and gets enhanced as Λ increases, under the combined effect of the temperature and greybody profiles. The spectrum for the bare temperature T_0 , starting from significant values for low Λ , is again monotonically suppressed as Λ increases approaching its maximum critical value. The spectra for all effective temperatures start from extremely low values and only the one for T_{eff-} manages to reach non-negligible values – this takes place only near the critical limit where T_{eff-} acquires a constant value. If we allow for a larger value of the number of extra dimensions, i.e. $n = 5$, the general behaviour of the emission curves

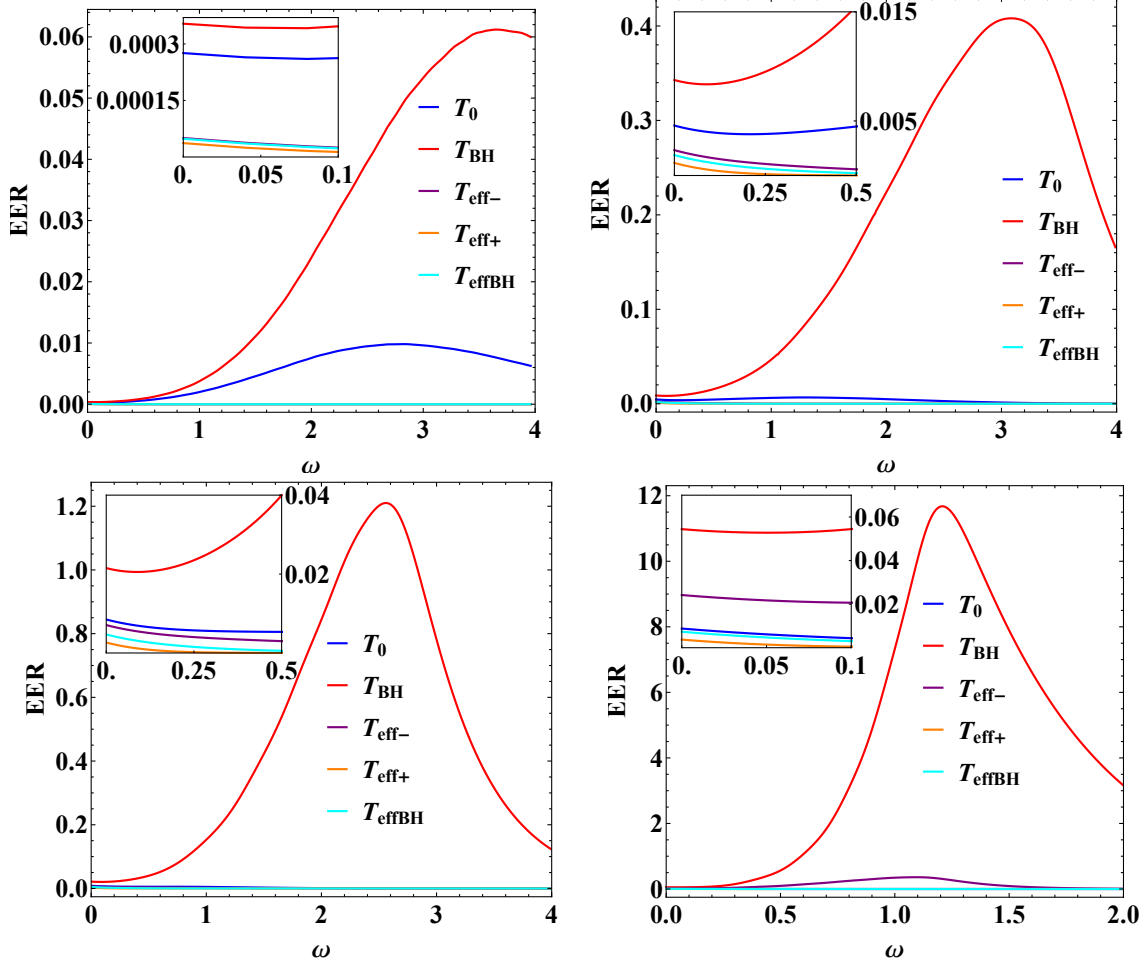


Figure 6: Energy emission rates for scalar fields in the bulk from a 9-dimensional ($n = 5$) Schwarzschild-de Sitter black hole for different temperatures T , and for: (a) $\Lambda = 4$, (b) $\Lambda = 10$, (c) $\Lambda = 13$ and (d) $\Lambda = 18$ (in units of r_h^{-2}).

remains the same, as can be seen from the plots in Fig. 6, drawn for four different values of the cosmological constant. Here, the additional suppression of all effective temperatures with n keeps even more the corresponding radiation spectra at low values.

Also in the bulk, all emission curves tend to a non-vanishing value in the limit $\omega \rightarrow 0$. This is again due to the non-zero asymptotic value of the greybody factor at the very low-energy regime. However, this value for bulk emission is [38]

$$|A^2| = \frac{4(r_h r_c)^{(n+2)}}{(r_c^{n+2} + r_h^{n+2})^2} + \mathcal{O}(\omega). \quad (33)$$

The above expression is suppressed with the number of extra dimensions n and this is the reason why this feature is more difficult to discern in the 9-dimensional emission curves of Fig. 6 compared to the 6-dimensional ones of Fig. 5 – it is nevertheless visible in the zoom-in plots that have been added in Fig. 6.

The numerical analysis performed in the context of the present work serves not only

as a comparison of the radiation emission curves when different expressions for the temperature of the SdS spacetime are used, but also as an extension to the previous results obtained in [43] where the normalised temperature T_{BH} was employed. There, exact results for the radiation spectra were produced but the range of values of the cosmological constant was much more restricted, i.e. $\Lambda \in [0.01, 0.3]$, therefore, the regime of large values of Λ , including the critical limit, was never studied. Here, we have performed a thorough analysis of the Λ regime for all different temperatures, and thus we have the complete picture of how the corresponding radiation spectra behave as a function of the value of the cosmological constant.

Overall, after having performed both the brane and the bulk analysis, we may conclude that it is the black-hole temperatures T_0 and T_{BH} that lead to Hawking radiation emission curves with the typical shape, i.e. start from a low value at the low-energy regime, rise to a maximum height and then slowly die out at the high-energy regime. In fact, even the T_0 spectrum loses this typical shape as Λ increases. Of the effective temperatures, only T_{eff-} manages to mimic this behaviour, and does so only close to the critical limit.

If we focus on the most typical radiation spectra, i.e. the ones derived for the normalised temperature T_{BH} , we could comment on some additional features that emerge from the more thorough study, in terms of the Λ -regime, performed in the present work. Our current results have confirmed the enhancement of the corresponding radiation spectra in terms of both the number of extra dimensions n and the value of the cosmological constant, as found in [43]. As Λ increases, the non-zero asymptotic value of each curve in the limit $\omega \rightarrow 0$ is enhanced thus increasing the probability of the emission of very low-energetic particles. In addition, for large values of n , as Λ increases, all emission curves, for brane and bulk propagation alike, show a significant shift of the peak of the curves towards the lower part of the spectrum. Therefore, we may conclude that the presence of a cosmological constant gives a significant boost to both low and intermediate-energy free, massless scalar particles and it does so more effectively the larger the number of extra dimensions is.

Finally, in [43] it was found that for Λ in the regime $[0.01, 0.3]$, the brane emission channel for free, massless scalar fields is always dominant compared to the bulk channel. Here, we observe that for larger values of Λ the situation is radically changed: even for small values of n , i.e. $n = 2$, the comparison of the vertical axes of the plots of Figs. 3 and 5 reveals that the bulk emission curve has surpassed, by a factor of two, the brane one, for values of Λ larger than 4. As the dimensionality of spacetime increases, the bulk dominance becomes more important: for $n = 5$, the comparison of the vertical axes of the plots of Figs. 4 and 6, now tells us that the bulk dominates over the brane for values of $\Lambda > 10$, i.e. for more than half the allowed regime of values of the cosmological constant, by a factor that ranges between 3 and 20.

4 Hawking Radiation Spectra for Non Minimally-Coupled Scalar Fields

In this section, we will consider the case of scalar particles propagating either on the brane or in the bulk and having a non-minimal coupling to gravity. This coupling is realised through a quadratic function $\xi\Phi^2$, where ξ is a constant, multiplying the appropriate scalar curvature (with the value $\xi = 0$ corresponding to the minimal coupling). The reason for studying such a theory is two-fold: first, the presence of the non-minimal coupling acts as an effective mass term for the scalar field, therefore the effect of the mass on the radiation spectra may thus be studied; second, for large values of the coupling constant ξ , it was found that the enhancement of the radiation spectra with the cosmological constant – for the normalised temperature T_{BH} , that was also evident in the results of the previous section – changes to a suppression in the low-energy and intermediate-energy regimes [43]. It would thus be interesting to see what the effect of the non-minimal coupling would be on the radiation spectra over for the complete Λ regime and for different temperatures.

For a scalar field propagating in the bulk, its higher-dimensional action would read

$$S_\Phi = -\frac{1}{2} \int d^{4+n}x \sqrt{-G} [\xi\Phi^2 R_D + \partial_M\Phi \partial^M\Phi] , \quad (34)$$

where G_{MN} is again the higher-dimensional metric tensor defined in Eq. (3), and R_D the corresponding curvature given by the expression

$$R_D = \frac{2(n+4)}{n+2} \kappa_D^2 \Lambda , \quad (35)$$

in terms of the bulk cosmological constant. The equation of motion of the bulk scalar field now reads

$$\frac{1}{\sqrt{-G}} \partial_M \left(\sqrt{-G} G^{MN} \partial_N \Phi \right) = \xi R_D \Phi , \quad (36)$$

or, more explicitly,

$$\frac{1}{r^{n+2}} \frac{d}{dr} \left(hr^{n+2} \frac{dR}{dr} \right) + \left[\frac{\omega^2}{h} - \frac{l(l+n+1)}{r^2} - \xi R_D \right] R = 0 . \quad (37)$$

In the above we have decoupled the radial part of the equation by considering the same factorized ansatz, namely $\Phi(t, r, \theta_i, \varphi) = e^{-i\omega t} R(r) \tilde{Y}(\theta_i, \varphi)$, as in the previous section.

The action functional for a scalar field propagating on the brane background and having also a quadratic, non-minimal coupling to the scalar curvature, will have a form similar to Eq. (34). However, now the metric tensor G_{MN} will be replaced by the projected-on-the-brane one $g_{\mu\nu}$ given in Eq. (7), and the higher-dimensional Ricci scalar R_D by the four-dimensional one R_4 that is found to be [42]

$$R_4 = \frac{24\kappa_D^2 \Lambda}{(n+2)(n+3)} + \frac{n(n-1)\mu}{r^{n+3}} . \quad (38)$$

The equation for the radial part of the brane-localised, non-minimally coupled scalar field then follows from Eq. (37) by setting $n = 0$ and changing R_D with R_4 , and reads

$$\frac{1}{r^2} \frac{d}{dr} \left(hr^2 \frac{dR}{dr} \right) + \left[\frac{\omega^2}{h} - \frac{l(l+1)}{r^2} - \xi R_4 \right] R = 0. \quad (39)$$

Both equations (37) and (39) were solved analytically in [42] and numerically in [43]. As it is clear from both equations, the non-minimal coupling term acts as an effective mass term, therefore any increase in the coupling function ξ causes a suppression to the radiation spectra, in accordance to previous studies of massive scalar fields [84, 85, 86, 87]. In addition, in [43], it was found that as ξ exceeds the value of approximately 0.3, any increase in the value of the cosmological constant causes a suppression in the low and intermediate part of the spectrum.

In the light of the above, here we will consider a value for the non-minimal coupling constant well beyond that critical value, namely we will choose $\xi = 1$. We will also study the complete Λ -regime and compute the radiation spectra for all five temperatures, T_0 , T_{BH} , T_{eff-} , T_{eff+} , and T_{effBH} . We will use again the exact numerical results for the brane and bulk greybody factors, that follow from an analysis identical to that in the minimal-coupling case – although the coupling constant ξ modifies the form of the effective potentials that the brane and bulk scalar fields have to overcome to reach infinity [42], it has no effect at the asymptotic regimes of the two horizons; therefore, the asymptotic solutions (24) and (28) as well as the boundary conditions (26)-(27) remain the same.

Starting from the emission of non-minimally-coupled scalar fields on the brane, in Fig. 7 we depict the differential energy emission rates for a 6-dimensional SdS black hole, and for the values $\Lambda = 2, 2.8, 4$ and 5 of the bulk cosmological constant. We first note that, in the presence of ξ , the emission curves have returned to their typical shape: as was found in [41, 42], and confirmed also here, the non-minimal coupling destroys the non-zero asymptotic limit of the scalar greybody factor in the low-energy limit; as a result, all emission curves emanate from zero at the low-energy regime. Moreover, the larger the value of ξ , the later in terms of ω the emission curves rise above the zero value, in accordance to the effect that the mass of the scalar particle has on the spectra [86, 87]. Also, by comparing the vertical axes of Figs. 3(b,c) and 7(a,c), respectively, we observe that the radiation spectra in the non-minimal case are indeed significantly suppressed, in accordance to the previous discussion.

This suppression is due to the fact that the greybody factors for both brane and bulk scalar fields decrease with any increase in the non-minimal coupling constant ξ , and therefore is common to the radiation spectra for the different temperatures. As a result, the inclusion of the non-minimal coupling does not modify the general picture drawn in the previous section. However, some of the radiation spectra are more sensitive to the changes brought by the presence of the non-minimal coupling. For example, in Fig. 3 drawn for the minimal-coupling case, we observe that, for the three effective temperatures and T_0 , the maxima of all emission curves are located at the very low-energy limit; the relatively small magnitude of these temperatures, compared to that of T_{BH} , combined with the enhanced value of the greybody factor for ultra soft particles,

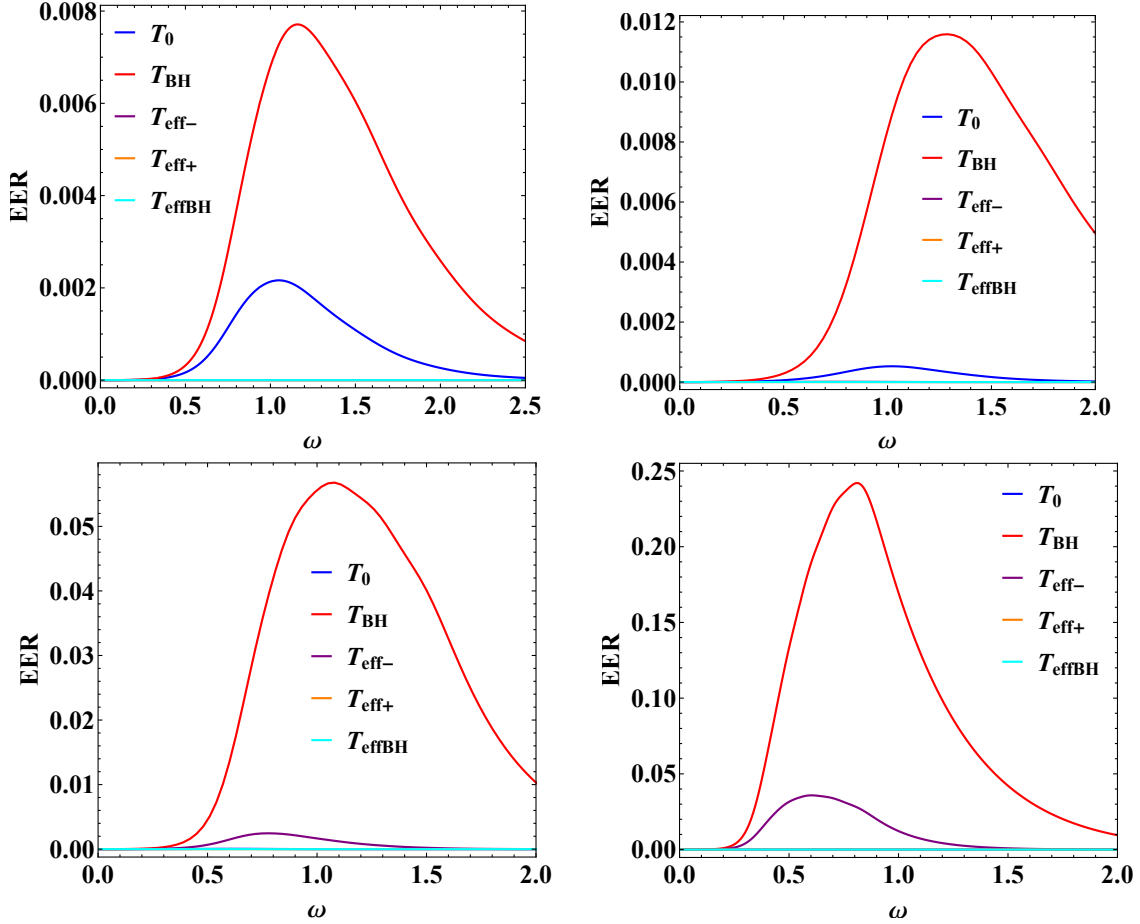


Figure 7: Energy emission rates for non-minimally coupled brane scalar fields, with $\xi = 1$, from a 6-dimensional ($n = 2$) SdS black hole for different temperatures T , and for: **(a)** $\Lambda = 2$, **(b)** $\Lambda = 2.8$, **(c)** $\Lambda = 4$ and **(d)** $\Lambda = 5$ (in units of r_h^{-2}).

makes the emission of low-energetic particles much more favourable for the black hole. When the non-minimal coupling is introduced, the emission of soft particles becomes disfavoured and the radiation spectra for the aforementioned four temperatures are significantly suppressed. The radiation spectrum for the normalised temperature T_{BH} is also suppressed, however its relatively large value allows also for the significant emission of higher-energetic particles and these are not significantly affected by the non-minimal coupling. As a result, the relative enhancement of the T_{BH} radiation spectrum compared to the remaining ones is extended by the non-minimal coupling. As the critical limit is approached, only the T_{eff-} spectrum manages again to reach comparable values due to its asymptotic, non-zero value at that regime.

A similar behaviour is observed also in the case where the number of extra dimensions takes larger values. We have performed the same analysis for $n = 5$, and found that all emission curves for non-minimally coupled brane scalar fields return again to their typical shape and thus have the emission of low-energy particles suppressed. For small values of Λ , and due to the enhancement with n that characterizes both T_0 and T_{BH} (see Fig. 2)

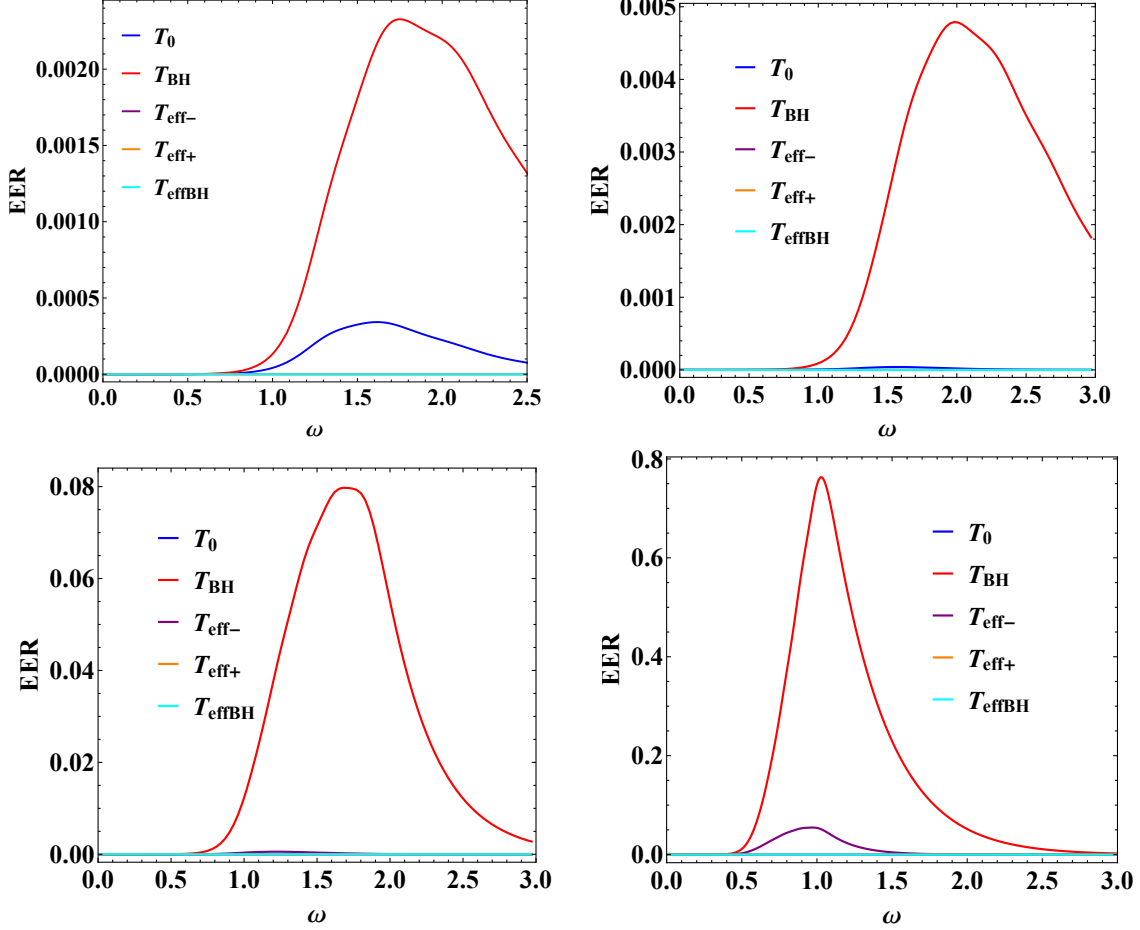


Figure 8: Energy emission rates for non-minimally coupled bulk scalar fields, with $\xi = 1$, from a 6-dimensional ($n = 2$) SdS black hole for different temperatures T , and for: (a) $\Lambda = 2$, (b) $\Lambda = 2.8$, (c) $\Lambda = 4$ and (d) $\Lambda = 5$ (in units of r_h^{-2}).

the difference in the corresponding two radiation spectra is smaller compared to the case with $n = 2$; as Λ however increases, the T_0 radiation spectrum is constantly suppressed reaching a negligible value at the critical limit. Of the effective temperature, only T_{eff-} manages to support a relatively significant spectrum and that is realised very close to the critical limit.

We now turn to the case of the emission of non-minimally-coupled scalar fields emitted in the bulk. The radiation spectra for the different temperatures and for the case with $n = 2$ are now depicted in Fig. 8, again for the value $\xi = 1$ and for the same four values of the cosmological constant. A similar picture emerges also here: the T_0 radiation spectrum is significant only in the low Λ regime, the T_{eff-} becomes important near the critical limit, while the other two radiation spectra for T_{eff+} and T_{effBH} fail to acquire any significant value at any Λ regime. The radiation spectrum for T_{BH} is the one that dominates over the whole energy regime and for the entire Λ range. The same behaviour is observed also for $n = 5$.

Let us finally note that the dominance of the bulk emission channel in the large Λ regime [43] is confirmed also in the case of non-minimal coupling and even for models with a small number of extra dimensions. As the comparison of the vertical axes of Figs. 7 and 8 reveals, the differential energy emission rate in the bulk exceeds that on the brane as soon as Λ becomes approximately larger than 3, and stays dominant for the remaining half of the allowed range.

5 Bulk-over-Brane Relative Emissivities

A final question that we would like to address in this section is that of the effect of the different temperatures on the total emissivities in the bulk and on the brane, and more particularly on the bulk-over-brane emissivity ratio. In our previous work [43], we calculated the total power emitted by the SdS black hole over the whole frequency range in both the brane and bulk channels, by employing the Bousso-Hawking T_{BH} normalization for the temperature. Here, we generalise this analysis to cover all five temperatures T_0 , T_{BH} , T_{eff-} , T_{eff+} and T_{effBH} , and compare the corresponding results. We also extend our previous study by considering the whole range of values for the bulk cosmological constant, from a vanishing value up to its critical limit.

The quantity of interest, namely the ratio of the total power emitted in the bulk over the corresponding total power on the brane, for the case with $n = 2$ and for four different values of the coupling constant ξ , i.e. $\xi = 0, 0.5, 1, 2$, is presented in Tables 1 through 4. The five columns of each Table give the total ratio for five values of the cosmological constant that span the entire allowed range, i.e. for $\Lambda = 0.3, 1, 2, 4, 5$. Let us see first how the change in the value of Λ affects our results. For small values of Λ , and independently of the value of ξ , the brane emission channel clearly dominates over the bulk one; however, as Λ increases, the bulk emission channel gradually becomes more and more important. This is due to the fact that for an increasing cosmological constant the bulk emission curves move to the right, thus allowing for the emission of a larger number of high-energetic particles compared to that on the brane, but also the maximum height of the bulk curves soon overpasses the one of the brane curves by a factor of 3. For the T_{BH} and T_{eff-} temperatures, that retain a significant value near the critical limit, the bulk-over-brane ratio well exceeds unity thus rendering the bulk channel the dominant one in the emission process of the black hole - the tendency of T_{BH} to overturn the power ratio in favour of the bulk channel was already anticipated by the results of [43]. The only exception to the above behaviour is the one exhibited by the bare temperature T_0 : the enhancement of the bulk-over-brane ratio with Λ is observed only in the case of minimal coupling whereas this ratio decreases for all values $\xi \neq 0$, as Λ increases towards its critical value. We may interpret this as the result of the disappearance of the low-energy modes as soon as the coupling constant ξ takes a non-vanishing value: the emission curves for T_0 have their maxima at the low-energy regime and are thus mostly affected when these are banned from the emission spectrum - according to our results, this change affects more the bulk channel rather than the brane one causing the suppression of the bulk-over-brane ratio.

If we now turn our attention to the role of the non-minimal coupling constant ξ in the

Table 1: Bulk over brane total emissivity for $n = 2$ and $\xi = 0$

$\Lambda \rightarrow$	0.3	1	2	4	5
T_0	0.259268	0.304247	0.402190	0.663547	0.781833
T_{BH}	0.338245	0.506324	0.798603	1.929660	3.247190
T_{eff-}	0.032997	0.132329	0.319508	0.860880	2.071590
T_{eff+}	0.032507	0.125599	0.298895	0.717772	0.884068
T_{effBH}	0.032950	0.130510	0.309000	0.669669	0.792598

Table 2: Bulk over brane total emissivity for $n = 2$ and $\xi = 0.5$

$\Lambda \rightarrow$	0.3	1	2	4	5
T_0	0.281627	0.220836	0.160691	0.089933	0.067954
T_{BH}	0.369359	0.450873	0.629061	1.617200	2.962410
T_{eff-}	0.003762	0.012441	0.038311	0.432708	1.710000
T_{eff+}	0.003424	0.008841	0.014009	0.019979	0.021436
T_{effBH}	0.003725	0.011167	0.022578	0.046074	0.052124

Table 3: Bulk over brane total emissivity for $n = 2$ and $\xi = 1$

$\Lambda \rightarrow$	0.3	1	2	4	5
T_0	0.286455	0.165240	0.089413	0.032550	0.020609
T_{BH}	0.380420	0.387464	0.500779	1.364060	2.704060
T_{eff-}	0.001233	0.003214	0.011410	0.279735	1.433260
T_{eff+}	0.001140	0.002529	0.003787	0.005227	0.005582
T_{effBH}	0.001222	0.002907	0.005497	0.012099	0.013918

Table 4: Bulk over brane total emissivity for $n = 2$ and $\xi = 2$

$\Lambda \rightarrow$	0.3	1	2	4	5
T_0	0.280978	0.099559	0.035998	0.007446	0.003698
T_{BH}	0.382963	0.287373	0.331984	1.002190	2.289020
T_{eff-}	0.000222	0.000471	0.001935	0.138896	1.045890
T_{eff+}	0.000216	0.000410	0.000580	0.000778	0.000828
T_{effBH}	0.000221	0.000438	0.000738	0.001767	0.002089

value of the bulk-over-brane ratio, we find that the overall behaviour is a suppression of this quantity as ξ increases. This behaviour holds for almost all values of the cosmological constant apart from the lower part of its allowed regime where, in contrast, the bulk-over-brane ratio exhibits an enhancement without however exceeding unity. On the other hand, despite the suppression with ξ , the bulk-over-brane ratio retains values above unity when Λ tends to its critical limit.

When we increase the number of the extra dimensions, all the above effects become amplified. In Tables 5 through 8, we display the value of the bulk-over-brane ratio for the case with $n = 5$, for the same four values of the non-minimal coupling constant ξ and for

Table 5: Bulk over brane total emissivity for $n = 5$ and $\xi = 0$

$\Lambda \rightarrow$	1	4	10	13	18
T_0	0.296070	0.299653	0.357216	0.422606	0.584868
T_{BH}	0.419245	0.818056	2.578580	4.629670	14.18230
T_{eff-}	0.000267	0.010603	0.140588	0.328066	4.192670
T_{eff+}	0.000265	0.010319	0.137045	0.291825	0.658816
T_{effBH}	0.000267	0.010549	0.134856	0.273098	0.559205

Table 6: Bulk over brane total emissivity for $n = 5$ and $\xi = 0.5$

$\Lambda \rightarrow$	1	4	10	13	18
T_0	0.468836	0.288097	0.099659	0.054591	0.016835
T_{BH}	0.641474	0.841435	1.770690	3.060490	11.19970
T_{eff-}	$3.152 \cdot 10^{(-6)}$	0.000090	0.002028	0.018275	2.231760
T_{eff+}	$2.898 \cdot 10^{(-6)}$	0.000071	0.000552	0.000923	0.001500
T_{effBH}	$3.139 \cdot 10^{(-6)}$	0.000086	0.000938	0.002127	0.005982

Table 7: Bulk over brane total emissivity for $n = 5$ and $\xi = 1$

$\Lambda \rightarrow$	1	4	10	13	18
T_0	0.664875	0.248447	0.040067	0.015499	0.002610
T_{BH}	0.890165	0.778299	1.195190	2.049140	9.026680
T_{eff-}	$3.679 \cdot 10^{(-7)}$	0.000007	0.000200	0.003575	1.293840
T_{eff+}	$3.956 \cdot 10^{(-7)}$	0.000006	0.000054	0.000095	0.000164
T_{effBH}	$3.683 \cdot 10^{(-7)}$	0.000007	0.000080	0.000187	0.000616

Table 8: Bulk over brane total emissivity for $n = 5$ and $\xi = 2$

$\Lambda \rightarrow$	1	4	10	13	18
T_0	1.162700	0.179527	0.009087	0.002170	0.000160
T_{BH}	1.509360	0.632852	0.585960	1.010350	6.207500
T_{eff-}	0.000274	$1.054 \cdot 10^{(-6)}$	$6.508 \cdot 10^{(-6)}$	0.000305	0.514108
T_{eff+}	0.000299	$1.653 \cdot 10^{(-6)}$	$1.827 \cdot 10^{(-6)}$	$3.402 \cdot 10^{(-6)}$	$6.292 \cdot 10^{(-6)}$
T_{effBH}	0.000275	$1.033 \cdot 10^{(-6)}$	$2.328 \cdot 10^{(-6)}$	$5.573 \cdot 10^{(-6)}$	0.000022

five indicative values of the bulk cosmological constant, i.e. $\Lambda = 1, 4, 10, 13$ and 18 , that again span the entire allowed regime. The dominance of the bulk channel over the brane one for T_{BH} and T_{eff-} , as Λ approaches its critical limit, is now much more prominent with the overall energy emitted in the bulk surpassing the one emitted on the brane by a factor of even larger than 10. The suppression of the energy ratio as ξ increases is also obvious here, but again this suppression does not prevent the bulk from becoming the dominant channel at the critical limit. What is different in this case from the $n = 2$ case is that the enhancement with ξ for small values of the cosmological constant, noted also in the case with $n = 2$, is now adequate to cause the dominance of the bulk channel

over the brane one for the bare T_0 and normalised T_{BH} temperatures - for the latter temperature, this effect was also observed in [43].

6 Conclusions

Over the years, the study of the thermodynamics of the Schwarzschild-de Sitter spacetime has proven to be a challenging task. The existence of two different horizons, the black-hole and the cosmological one – each with its own temperature expressed in terms of its surface gravity – results into the absence of a true thermodynamical equilibrium. On the other hand, the absence of an asymptotically-flat limit led to the formulation of a normalised temperature for the black hole [51] more than two decades ago. Both problems become more severe in the limit of large cosmological constant when the two horizons are located so close to each other that the argument of the two independent thermodynamics, valid at the two horizons, comes into question. As a result, the notion of the effective temperature of the SdS spacetime was proposed [53, 54, 55, 56] that implements both the black-hole and the cosmological horizon temperatures.

In the context of the present work, we have focused on the case of the higher-dimensional Schwarzschild-de Sitter black hole, and have formed a set of five different temperatures: the bare black-hole temperature T_0 , based on its surface gravity, the normalised black-hole temperature T_{BH} and three effective temperatures for the SdS spacetime, T_{eff-} , T_{eff+} and T_{effBH} – the latter three are inspired by four-dimensional analyses, where the cosmological constant plays the role of the pressure of the system, and are combinations of the black-hole and cosmological horizon temperatures. We have first studied the dependence of the aforementioned temperatures on the value of the cosmological constant, as this is varied from zero to its maximum allowed value, set by the critical limit where the two horizons coincide. In the limit of vanishing cosmological constant, the black-hole temperatures T_0 and T_{BH} reduce to the temperature of an asymptotically-flat, higher-dimensional Schwarzschild black hole as expected; on the other hand, all three effective temperatures tend to zero, an artificially ill behaviour due to the fact that Λ (or, equivalently the pressure of the system) is not allowed to vanish. In the opposite limit, that of the critical value, it is the normalised T_{BH} and effective T_{eff-} temperatures that have a common behaviour reaching a non-vanishing asymptotic value; the other three temperatures all vanish in the same limit. We then examined the dependence of the temperatures on the number of extra dimensions. Here, the five temperatures were found to fall again into two categories: the black-hole temperatures T_0 and T_{BH} both are enhanced with n while all effective temperatures predominantly are suppressed. Overall, the normalised T_{BH} temperature was found to be the dominant one for all values of Λ and n .

The set of five temperatures was then used to derive the Hawking radiation spectra for a free, massless scalar field propagating both on the brane and in the bulk. We considered the cases where the number of extra dimensions had a small ($n = 2$) and a large ($n = 5$) value: in each case, we chose four different values for the cosmological constant that covered the allowed regime from zero to the critical value. For both brane and bulk radiation spectra, the emission curves closely followed the behaviour of the tempera-

tures: for small Λ , the emission curves for all effective temperatures were significantly suppressed while the ones for the black-hole temperatures were the dominant ones. As Λ increased, the emission rate for the bare T_0 started to become suppressed while the one for the effective T_{eff-} started to become important. Near the critical limit, it is the two temperatures, T_{BH} and T_{eff-} , with the non-vanishing values that lead to the dominant emission curves. It is worth noting that the two effective temperatures T_{eff+} and T_{effBH} support a non-negligible emission rate only for intermediate values of the cosmological constant, where they favour the emission of very low-energetic scalar particles. The emission rate for the normalised temperature T_{BH} is the one that constantly rises as Λ gradually increases, being clearly the dominant one: for $n = 2$, the peak of the emission curve on the brane for T_{BH} rises to a height that is 2 times larger than that for T_0 at the low Λ -regime and 5 times larger than that for T_{eff-} at the high Λ -regime; these factors increase even more as n increases, or when we study the bulk emission channel.

For the case of a minimally-coupled scalar field, all emission curves were found to have non-zero asymptotic values at the very-low part of the spectrum due to the well-known behaviour of the greybody factor both on the brane and in the bulk. As a result, a significant number of soft particles are expected to be emitted; in fact, for the three effective temperatures T_{eff-} , T_{eff+} , T_{effBH} (for small values of values of Λ) and for T_0 (for large values of Λ) this is where the peak of the emission curves is located. When the non-minimal coupling to the scalar curvature is turned on, the emission curves for all five temperatures resume their usual shape. The general behaviour regarding the comparative strength of the emission curves for the different temperatures observed in the case of the minimal coupling holds also here. The emission curve for the normalised temperature T_{BH} is again the dominant one over the entire Λ -regime, with only the emission curves for T_0 and T_{eff-} reaching significant values at low and large values of Λ , respectively.

The exact analysis performed in the context of this work serves not only as a comparison of the radiation spectra, that follow by using different temperatures for the Schwarzschild-de Sitter spacetime, but also as a source of information regarding their behaviour as the cosmological constant varies from a very small value to the largest allowed one at the critical limit. The complete radiation spectra reveal that as Λ increases, the emission of energy from the black hole along the brane and bulk channels very quickly become comparable, and even for low values of the number of extra dimensions, the bulk emission eventually dominates over the brane one. The exact total emissivities that were calculated in Section 5 demonstrated exactly this effect: apart from the case of T_0 when $\xi \neq 0$, the bulk-over-brane ratio exhibits a significant enhancement as Λ increases and, in fact, renders the bulk channel the dominant emission channel of the SdS black hole for the temperatures T_{BH} and T_{eff-} , i.e. for the temperatures that retain a non-vanishing value near the critical limit. In addition, when the number of extra dimensions is large enough, the bulk was found to dominate over the brane even for values of Λ much lower than its critical limit as long as the value of the non-minimal coupling constant ξ was large enough; in this case, the bulk dominance was obtained also for the bare temperature T_0 .

In conclusion, choosing a particular form for the temperature of an SdS black hole, i.e. the bare, the normalised or an effective one, plays a paramount role in the form of

the obtained radiation spectra. Some of the suggested temperatures fail even to produce a significant emission rate, others lead to an emission only for very small or very large values of the bulk cosmological constant. Our results clearly reveal that the normalised temperature T_{BH} , the one that makes amends for the absence of an asymptotically-flat limit in a Schwarzschild-de Sitter spacetime, is the one that produces the most robust radiation spectra over the entire regime of the bulk cosmological constant.

Acknowledgement T.P. would like to thank the Alexander S. Onassis Public Benefit Foundation for financial support.

References

- [1] N. Arkani-Hamed, S. Dimopoulos and G. R. Dvali, Phys. Lett. B **429**, 263 (1998); Phys. Rev. D **59**, 086004 (1999); I. Antoniadis, N. Arkani-Hamed, S. Dimopoulos and G. R. Dvali, Phys. Lett. B **436**, 257 (1998).
- [2] L. Randall and R. Sundrum, Phys. Rev. Lett. **83** (1999) 3370; Phys. Rev. Lett. **83** (1999) 4690.
- [3] P. Kanti, Int. J. Mod. Phys. A **19**, 4899–4951 (2004).
- [4] M. Cavaglia, Int. J. Mod. Phys. A **18** (2003) 1843.
- [5] G. L. Landsberg, Eur. Phys. J. C **33**, S927–S931 (2004).
- [6] A. S. Majumdar and N. Mukherjee, Int. J. Mod. Phys. D **14**, 1095–1129 (2005).
- [7] S. C. Park, Prog. Part. Nucl. Phys. **67**, 617–650 (2012).
- [8] B. Webber, eConf C **0507252**, T030 (2005) [hep-ph/0511128].
- [9] A. Casanova and E. Spallucci, Class. Quant. Grav. **23**, R45–R62 (2006).
- [10] P. Kanti, Lect. Notes Phys. **769**, 387–423 (2009).
- [11] P. Kanti, Rom. J. Phys. **57**, 879–893 (2012).
- [12] E. Winstanley, arXiv:0708.2656 [hep-th] (2007).
- [13] P. Kanti, J. Phys. Conf. Ser. **189**, 012020 (2009).
- [14] P. Kanti and E. Winstanley, arXiv:1402.3952 [hep-th].
- [15] S. W. Hawking, Commun. Math. Phys. **43**, 199–220 (1975)
- [16] F. R. Tangherlini, Nuovo Cim. **27** (1963) 636.
- [17] P. Kanti and J. March-Russell, Phys. Rev. D **66**, 024023 (2002); Phys. Rev. D **67**, 104019 (2003).
- [18] C. M. Harris and P. Kanti, JHEP **0310**, 014 (2003).

- [19] A. S. Cornell, W. Naylor and M. Sasaki, JHEP **0602**, 012 (2006);
V. Cardoso, M. Cavaglia and L. Gualtieri, Phys. Rev. Lett. **96**, 071301 (2006); JHEP **0602**, 021 (2006);
S. Creek, O. Efthimiou, P. Kanti and K. Tamvakis, Phys. Lett. B **635**, 39 (2006).
- [20] C. M. Harris and P. Kanti, Phys. Lett. B **633** (2006) 106;
G. Duffy, C. Harris, P. Kanti and E. Winstanley, JHEP **0509**, 049 (2005).
- [21] M. Casals, P. Kanti and E. Winstanley, JHEP **0602**, 051 (2006).
- [22] M. Casals, S. Dolan, P. Kanti and E. Winstanley, JHEP **0703**, 019 (2007); JHEP **0806**, 071 (2008).
- [23] D. Ida, K. y. Oda and S. C. Park, Phys. Rev. D **67**, 064025 (2003) [Erratum-ibid. D **69**, 049901 (2004)]; Phys. Rev. D **71**, 124039 (2005); Phys. Rev. D **73**, 124022 (2006).
- [24] S. Creek, O. Efthimiou, P. Kanti and K. Tamvakis, Phys. Rev. D **75** (2007) 084043;
Phys. Rev. D **76** (2007) 104013; Phys. Lett. B **656**, 102 (2007).
- [25] V. P. Frolov and D. Stojkovic, Phys. Rev. D **67**, 084004 (2003);
H. Nomura, S. Yoshida, M. Tanabe and K. i. Maeda, Prog. Theor. Phys. **114**, 707 (2005);
E. Jung and D. K. Park, Nucl. Phys. B **731**, 171 (2005); Mod. Phys. Lett. A **22**, 1635 (2007);
S. Chen, B. Wang, R. K. Su and W. Y. Hwang, JHEP **0803**, 019 (2008).
- [26] H. Kodama, Prog. Theor. Phys. Suppl. **172**, 11 (2008); Lect. Notes Phys. **769**, 427 (2009);
J. Doukas, H. T. Cho, A. S. Cornell and W. Naylor, Phys. Rev. D **80** (2009) 045021;
P. Kanti, H. Kodama, R. A. Konoplya, N. Pappas and A. Zhidenko, Phys. Rev. D **80** (2009) 084016.
- [27] A. Flachi, M. Sasaki and T. Tanaka, JHEP **0905** (2009) 031.
- [28] M. Casals, S. R. Dolan, P. Kanti and E. Winstanley, Phys. Lett. B **680** (2009) 365.
- [29] D. C. Dai and D. Stojkovic, JHEP **1008** (2010) 016.
- [30] M. O. P. Sampaio, JHEP **1203** (2012) 066.
- [31] J. Grain, A. Barrau and P. Kanti, Phys. Rev. D **72** (2005) 104016.
- [32] V. P. Frolov and D. Stojkovic, Phys. Rev. D **66**, 084002 (2002); Phys. Rev. Lett. **89**, 151302 (2002);
D. Stojkovic, Phys. Rev. Lett. **94**, 011603 (2005).
- [33] D. C. Dai, N. Kaloper, G. D. Starkman and D. Stojkovic, Phys. Rev. D **75**, 024043 (2007);
T. Kobayashi, M. Nozawa, Y. Takamizu, Phys. Rev. D **77**, 044022 (2008).

- [34] R. Jorge, E. S. de Oliveira and J. V. Rocha, *Class. Quant. Grav.* **32**, no. 6, 065008 (2015).
- [35] R. Dong and D. Stojkovic, *Phys. Rev. D* **92**, no. 8, 084045 (2015).
- [36] G. Panotopoulos and A. Rincon, arXiv:1611.06233 [hep-th].
- [37] Y. G. Miao and Z. M. Xu, arXiv:1704.07086 [hep-th].
- [38] P. Kanti, J. Grain and A. Barrau, *Phys. Rev. D* **71** (2005) 104002.
- [39] T. Harmark, J. Natario and R. Schiappa, *Adv. Theor. Math. Phys.* **14** (2010) 727.
- [40] S. F. Wu, S. y. Yin, G. H. Yang and P. M. Zhang, *Phys. Rev. D* **78**, 084010 (2008).
- [41] L. C. B. Crispino, A. Higuchi, E. S. Oliveira and J. V. Rocha, *Phys. Rev. D* **87** (2013) 10, 104034.
- [42] P. Kanti, T. Pappas and N. Pappas, *Phys. Rev. D* **90**, no. 12, 124077 (2014).
- [43] T. Pappas, P. Kanti and N. Pappas, *Phys. Rev. D* **94** (2016) no.2, 024035.
- [44] P. R. Anderson, A. Fabbri and R. Balbinot, *Phys. Rev. D* **91**, no. 6, 064061 (2015).
- [45] C. A. Sporea and A. Borowiec, *Int. J. Mod. Phys. D* **25**, no. 04, 1650043 (2016).
- [46] J. Ahmed and K. Saifullah, arXiv:1610.06104 [gr-qc].
- [47] S. Fernando, arXiv:1611.05337 [gr-qc].
- [48] P. Boonserm, T. Ngampitipan and P. Wongjun, arXiv:1705.03278 [gr-qc].
- [49] G. W. Gibbons and S. W. Hawking, *Phys. Rev. D* **15** (1977) 2738.
- [50] G. W. Gibbons and S. W. Hawking, *Phys. Rev. D* **15** (1977) 2752.
- [51] R. Bousso and S. W. Hawking, *Phys. Rev. D* **54** (1996) 6312.
- [52] S. Shankaranarayanan, *Phys. Rev. D* **67** (2003) 084026.
- [53] M. Urano, A. Tomimatsu and H. Saida, *Class. Quant. Grav.* **26** (2009) 105010.
- [54] S. Bhattacharya and A. Lahiri, *Eur. Phys. J. C* **73** (2013) 2673.
- [55] S. Bhattacharya, *Eur. Phys. J. C* **76** (2016) no.3, 112.
- [56] H. F. Li, M. S. Ma and Y. Q. Ma, *Mod. Phys. Lett. A* **32** (2017) no.02, 1750017 [arXiv:1605.08225 [hep-th]].
- [57] D. Kubiznak, R. B. Mann and M. Teo, *Class. Quant. Grav.* **34** (2017) no.6, 063001.
- [58] L. J. Romans, *Nucl. Phys. B* **383** (1992) 395.
- [59] D. Kastor and J. H. Traschen, *Phys. Rev. D* **47** (1993) 5370.

- [60] R. G. Cai, Phys. Lett. B **525** (2002) 331; Nucl. Phys. B **628** (2002) 375.
- [61] A. M. Ghezelbash and R. B. Mann, JHEP **0201** (2002) 005.
- [62] Y. Sekiwa, Phys. Rev. D **73** (2006) 084009.
- [63] M. Cvetič, G. W. Gibbons and C. N. Pope, Phys. Rev. Lett. **106** (2011) 121301.
- [64] B. P. Dolan, D. Kastor, D. Kubiznak, R. B. Mann and J. Traschen, Phys. Rev. D **87** (2013) no.10, 104017.
- [65] M. S. Ma, H. H. Zhao, L. C. Zhang and R. Zhao, Int. J. Mod. Phys. A **29** (2014) 1450050.
- [66] H. H. Zhao, L. C. Zhang, M. S. Ma and R. Zhao, Phys. Rev. D **90** (2014) no.6, 064018.
- [67] L. C. Zhang, M. S. Ma, H. H. Zhao and R. Zhao, Eur. Phys. J. C **74** (2014) no.9, 3052.
- [68] M. S. Ma, L. C. Zhang, H. H. Zhao and R. Zhao, Adv. High Energy Phys. **2015** (2015) 134815 doi:10.1155/2015/134815 [arXiv:1410.5950 [gr-qc]].
- [69] X. Guo, H. Li, L. Zhang and R. Zhao, Phys. Rev. D **91** (2015) no.8, 084009;
- [70] X. Guo, H. Li, L. Zhang and R. Zhao, Adv. High Energy Phys. **2016** (2016) 7831054.
- [71] A. Araujo and J. G. Pereira, Int. J. Mod. Phys. D **24** (2015) no.14, 1550099.
- [72] D. Kubiznak and F. Simovic, Class. Quant. Grav. **33** (2016) no.24, 245001.
- [73] J. McInerney, G. Satishchandran and J. Traschen, Class. Quant. Grav. **33** (2016) no.10, 105007.
- [74] H. F. Li, M. S. Ma, L. C. Zhang and R. Zhao, Nucl. Phys. B **920** (2017) 211.
- [75] H. Liu and X. h. Meng, arXiv:1611.03604 [gr-qc].
- [76] B. Pourhassan, S. Upadhyay and H. Farahani, arXiv:1701.08650 [physics.gen-ph].
- [77] H. Nariai, Sci. Rep. Tohoku Univ., I., 35 (1951) 62.
- [78] R. C. Myers and M. J. Perry, Annals Phys. **172**, 304 (1986).
- [79] C. Molina, Phys. Rev. D **68** (2003) 064007.
- [80] J. W. York, Jr., Phys. Rev. D **31** (1985) 775.
- [81] J. Labbe, A. Barrau and J. Grain, PoS HEP **2005** (2006) 013 [hep-ph/0511211].
- [82] M. Bander and C. Itzykson, Rev. Mod. Phys. **38**, 330 (1966).

- [83] C. Muller, in *Lecture Notes in Mathematics: Spherical Harmonics* (Springer-Verlag, Berlin-Heidelberg, 1966).
- [84] D. N. Page, Phys. Rev. D **16** (1977) 2402.
- [85] E. I. Jung, S. H. Kim and D. K. Park, Phys. Lett. B **586** (2004) 390; JHEP **0409** (2004) 005; Phys. Lett. B **602** (2004) 105.
- [86] M. O. P. Sampaio, JHEP **0910** (2009) 008; JHEP **1002** (2010) 042.
- [87] P. Kanti and N. Pappas, Phys. Rev. D **82** (2010) 024039.